

Measurements of the aeolian sand transport saturation length

B. Andreotti^a, P. Claudin^{a,*}, O. Pouliquen^b

^a Laboratoire de Physique et Mécanique des Milieux Hétérogènes (PMMH), UMR 7636 CNRS-ESPCI-Univ. P.M. Curie - Univ. Paris Diderot, 10 Rue Vauquelin, 75231 Paris Cedex 05, France

^b Institut Universitaire des Systèmes Thermiques Industriels (IUSTI), UMR 6595 CNRS-Univ. Provence, 5 rue Enrico Fermi, 13453 Marseille Cedex 13, France

ARTICLE INFO

Article history:

Received 3 July 2008

Received in revised form 19 July 2010

Accepted 1 August 2010

Available online 7 August 2010

Keywords:

Aeolian sediment transport

Sand flux saturation

Sand dunes

ABSTRACT

The wavelength at which a dune pattern emerges from a flat sand bed is controlled by the sediment transport saturation length, which is the length needed for the sand flux to adapt to a change in wind strength. The influence of the wind shear velocity on this saturation length and on the subsequent dune initial wavelength has remained controversial. In this paper, we present direct measurements of the saturation length performed in a wind tunnel experiment. Complementary to this, initial dune wavelengths are measured under different wind conditions – in particular after storms. Using the linear stability analysis of dune formation, it is then possible to deduce the saturation length from field data. Both direct and indirect measurements agree that the saturation length is almost independent of the wind strength. This result supports the idea that grain inertia is the dominant dynamical mechanism limiting sediment transport saturation on dunes.

© 2010 Elsevier B.V. All rights reserved.

1. Introduction

Understanding how wind transports sand is important in many geomorphological problems including dunes dynamics. It is well known that for a given wind shear velocity u_* greater than a threshold u_{th} , the sand flux q saturates to a steady value $q_{sat}(u_*, u_{th})$, which results from the interaction between the grains in motion and the wind velocity (Bagnold, 1941; Owen, 1964; Ungar and Haff, 1987; Andreotti, 2004). The transient regime and the way q adjusts to q_{sat} is still the source of some confusion. In particular, a situation in which external parameters (e.g. the basal shear stress or the bed roughness) vary, leading to a downwind drift of q_{sat} contrasts, in terms of the physics, with the spatial evolution of the flux due to internal relaxation processes.

If a change in shear velocity u_* takes place, the flux does not adjust instantaneously to its new equilibrium value, and a lag exists between q and u_* . Whatever the dynamical mechanisms responsible for this lag, it has been proposed to encode it into a single length L_{sat} , called the saturation length. By definition, L_{sat} is then the length over which the flux q relaxes to q_{sat} . Around the saturated regime, this relaxation can be modeled by a first order equation:

$$L_{sat} \frac{dq}{dx} = q_{sat} - q, \quad (1)$$

where x is the downstream coordinate (see Fig. 1). Different physical mechanisms can be responsible for this saturation length, e.g., the

grain hop length (Charru, 2006); the length needed to accelerate new grains (called the drag length) (Andreotti et al., 2002; Hersen et al., 2002; Andreotti and Claudin, 2007); the length needed to expel new grains from the sand bed (Sauermaun et al., 2001; Parteli et al., 2007); and the length needed for the negative feedback of transport on the wind to take place (Andreotti, 2004). Importantly, transport saturation is eventually limited by the slowest of these processes.

Understanding the physical origin of sand flux saturation is crucial in order to get a better description of the formation of dunes. Dunes result from the interaction between the wind and the topographic shape of the sand surface (Bagnold, 1941; Lancaster et al., 1996; Wiggs et al., 1996; McKenna-Neuman et al., 1997; Andreotti et al., 2002). Recent models have shown that the initial formation of dunes is controlled by the balance between three different mechanisms. The first one is the phase-lag between the dune elevation profile h and the basal shear velocity u_* (Jackson and Hunt, 1975; Hunt et al., 1988). This purely hydrodynamical mechanism, related to fluid inertia and dissipation, is the driver of the instability and tends to destabilise the bed (Richards, 1980; Andreotti et al., 2002; Elbelrhiti et al., 2005; Fourrière et al., 2010). On the other hand, two stabilizing effects exist. The dynamics of sediment transport tend to stabilise short wavelengths, due to the space-lag between sand flux q and shear velocity u_* . Gravity has a further stabilizing effect, related to the dependence of the threshold shear velocity u_{th} on the local slope (Rasmussen et al., 1996). A stability analysis taking into account these three components, (Andreotti and Claudin, 2007; Fourrière et al., 2010) shows that the most unstable wavelength is proportional to L_{sat} and decreases with u_*/u_{th} . Saturation length then controls the initial size of aeolian dunes.

Assuming that grain inertia is the dominant dynamical mechanism limiting saturation, one expects L_{sat} to be independent of the shear

* Corresponding author.

E-mail address: claudin@pmmh.espci.fr (P. Claudin).

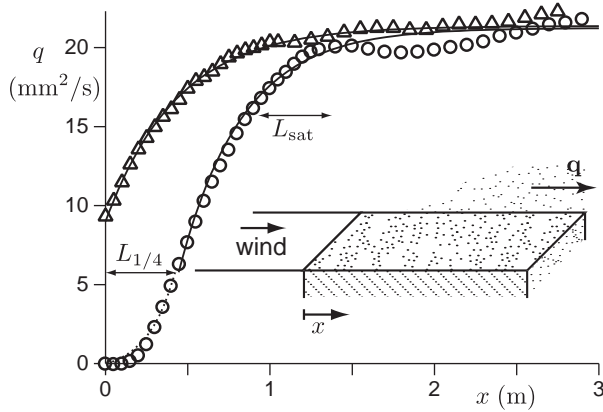


Fig. 1. Spatial variation of the sediment flux over a flat sand bed for $u_* = 0.33 \text{ m/s} \approx 1.5 u_{th}$, with (Δ) or without (\circ) an input flux. Solid lines: best exponential fit around the saturated state. Dotted lines: initial exponential increase. Inset: sketch of the experiments. The sand bed starts at $x=0$.

velocity and to scale with the drag length $L_{drag} \equiv \rho_s / \rho_f d$, where ρ_s and ρ_f are respectively the grain and fluid density, and d is the grain size. Under this assumption, a scaling law for the elementary size of dunes has been proposed (Claudin and Andreotti, 2006). Still, this assumption remains controversial (Sauermann et al., 2001; Andreotti and Claudin, 2007; Parteli et al., 2007).

In this paper, we aim to investigate the physical origin of the sand transport saturation length by studying its dependence on the wind strength. Two methods are used; a direct one by measuring the saturation of the sand flux in a wind tunnel, and an indirect method based on field measurements of the wavelength at which a sand bed first destabilises.

2. Wind tunnel measurements

We first report direct measurements of L_{sat} obtained from controlled experiments. They have been performed in the wind tunnel of the Cemagref in Grenoble (1 m wide, 0.5 m high, and 4.5 m long), using sand grains of diameter $d = 120 \pm 40 \mu\text{m}$ from Hostun quarry (Cierco et al., 2008). An initial 3 cm-thick sand bed is prepared and flattened with a moving bar. This thickness is gently matched to the wind tunnel rough bottom over the first ten centimetres (Fig. 1). The bed elevation profile $h(x, t)$ is measured at regular time interval with a vertical resolution of $500 \mu\text{m}$, turning off the flow. In most of the experiments, we observed that $h(x, t)$ varies linearly in time: $h(x, t) \approx h(x, 0) + \partial_t h(x)t$. In that case, the erosion rate profile $\partial_t h(x)$ is determined from four elevation profiles $h(x, t)$ (including the initial one). In the few cases where the measurements were not consistent with a well-defined erosion rate, we have performed the experiment a second time in the same conditions.

We define the mass flux q_m as the mass of grains crossing a unit length per unit time. Using the sand bed volume fraction ϕ_{bed} and the grain density ρ_s , both assumed to be uniform, we define the flux $q = q_m / (\rho_s \phi_{bed})$. q is a volume of sand (at the volume fraction of the bed) crossing a unit length per unit time. Using the conservation of mass, the sediment flux q at position x is simply deduced from the erosion data as:

$$q(x) = - \int_0^x \partial_t h(\xi) d\xi \quad (2)$$

Let us emphasize that this measurement method is much more precise than the methods based on sand traps. The density of transported grains decreases exponentially with height over a length-scale on the order of few cm (Liu and Dong, 2004; Creyssels et al., 2009); so, most of the sand traps do not have sufficient spatial resolution to measure the overall flux accurately. Similarly, most of

the former studies on the saturation process do not present the centimeter-scale horizontal resolution reached here.

Fig. 1 compares the profiles of the flux obtained with and without an input flux at the upstream bed entrance. In both cases, the sediment transport increases downstream and further saturates to the same value q_{sat} . The evolution of q can be divided into two phases: a first increase followed by a relaxation phase toward equilibrium. The initial phase is linked to ejection of grains, each saltating grain ejecting a few other grains when it collides with the bed. This results into an exponential increase of the flux (dotted lines in Figs. 1 and 2). This regime is *a priori* not taken into account in Eq. (1), which aims to describe the relaxation close to the saturated state. To determine the saturation length, we have thus analysed the zone where the flux is larger than one fourth of its saturated value q_{sat} . The solid lines in Figs. 1 and 2 show the best fits by an exponential law of the form $q_{sat}[1 - e^{-(x-x_0)/L_{sat}}]$, which is the solution of Eq. (1). This fit allows us to extract very precisely three parameters: the saturated flux q_{sat} , the saturation length L_{sat} and the position $x = L_{1/4}$ at which the flux reaches the value $q_{sat}/4$. Fig. 1 shows that the saturation length L_{sat} does not depend on the entrance condition.

It is worth emphasizing the difference between the saturation length L_{sat} and the fetch distance usually defined in the literature. Looking at Fig. 1, one could say that the transport takes 1 to 2 m to saturate, i.e. to reach a significant fraction of the saturated flux. However, this includes the initial ejection stage of length $L_{1/4}$, plus a part of the exponential relaxation to equilibrium. L_{sat} characterizes the final stage of the relaxation, which is the only one relevant for dune formation. As a matter of fact, we have estimated that the sand flux over real dunes is always within 20% of its saturated value. Note finally that L_{sat} is much shorter (typically 40 cm in Fig. 1) than the apparent fetch distance.

There is yet another difference between the saturation length and the fetch distance. Consider the transition between a vegetated area and a dust covered salt lake. Then, the basal shear velocity slowly increases in space over hundreds of meters. Then, the saturated flux q_{sat} is also varying on this length-scale so that the flux remains undersaturated over a large distance (Gilette et al., 1996). However, this distance has nothing to do with the sediment transport relaxation processes. Slow variations of the driving conditions (basal shear stress and roughness) may also be encountered. In the wind tunnel experiments presented here, we have systematically checked the saturation of the flux using a simple criterion: there exists a meter-scale region at the downstream end of the tunnel which is not eroded,

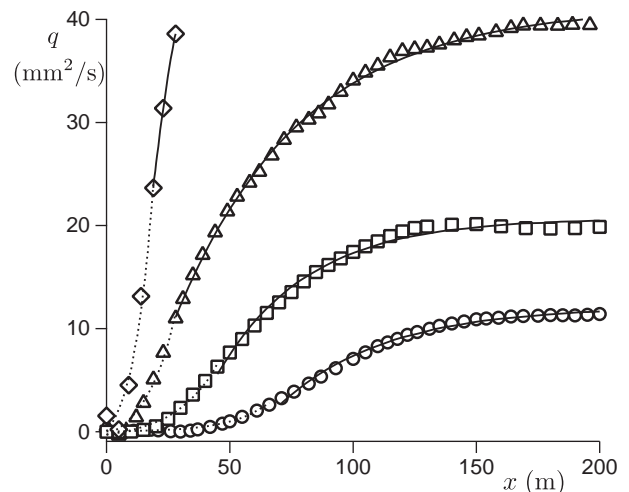


Fig. 2. Spatial variation of the sediment flux over a flat sand bed, measured in a wind tunnel for different wind speeds: $u_* = 0.26 \text{ m/s} \approx u_{th}$ (\circ), $u_* = 0.33 \text{ m/s} \approx 1.5 u_{th}$ (\square), $u_* = 0.39 \text{ m/s} \approx 1.8 u_{th}$ (\triangle) and $u_* = 0.48 \text{ m/s} \approx 2.2 u_{th}$ (\diamond). Solid lines: best exponential fit around the saturated state. Dotted lines: initial exponential increase.

within error bars – once the modulation of the surface by aeolian ripples is removed. This criterion was not fulfilled at very large wind velocity, where we have observed a progressive sorting of the sand covering the surface, the smallest grains being preferentially entrained. In that case, the experimental conditions slowly drift in space, which leads to a fetch distance much larger than the values of L_{sat} measured at low wind. The results presented here are thus limited to rather low wind velocities $u_* < 3u_{\text{th}}$ – but which is actually the relevant range for natural dunes.

The curves $q(x)$ obtained for different wind strengths are depicted in Fig. 2. As expected, the saturated flux q_{sat} increases with wind strength. The initial stage, where the flux increases exponentially, is noticeable for weak wind and becomes negligible at high wind. This means that the ejection of new sand grains becomes more and more efficient as the flow velocity increases. In contrast, the region of the saturation is remarkably insensitive to u_* . These qualitative observations are made quantitative by measuring both the length of the initial stage $L_{1/4}$ and the saturation length L_{sat} . One observes in Fig. 3 that $L_{1/4}$ diverges at the threshold and decreases very rapidly with u_* . In contrast, the saturation length L_{sat} is independent of u_* , within error bars. Its average is around 55 cm, with a standard deviation of 10 cm.

The saturation lengths measured here are significantly smaller than that ($L_{\text{sat}} \sim 2.3$ m) determined from the measurements of Bagnold (1941) (Fig. 62, p. 182) with grains of diameter $d = 240 \mu\text{m}$. This is probably due to the fact that the erosion rate was measured by means of spring balances below sections of the tunnel, of the size of the actual saturation length. Dong et al. (2004) has performed measurements for grains of diameter $d = 180 \mu\text{m}$, with a space resolution of 50 cm. The best fit by an exponential relaxation gives 70 cm for $u_* \approx 1.6 u_{\text{th}}$ and around 2.3 m in the range $u_*/u_{\text{th}} = 2-3$. Note that in these experiments, the height over which the sand flux decays is found to depend on the wind strength, contrarily to the measurements obtained in most experiments (see Creyssels et al. (2009) and references therein). By contrast to previous works, in our wind tunnel measurements, we have used a horizontal space resolution of 10 cm, which allows to measure accurately L_{sat} within 20%.

Fig. 4(a) displays a flux profile measured in the field by Elbelrhiti et al. (2005) in the Atlantic Sahara. A 20 m-long sand bed composed of grains of size $d = 185 \mu\text{m}$ was prepared using a bulldozer to flatten the bed. Erosion was measured after 24 h of wind fluctuating around the transport threshold. By fitting the curve $q(x)$ in the zone where $q > q_{\text{sat}}/4$, we find a saturation length of 1 ± 0.2 m, twice smaller than that obtained by fitting the whole profile (1.7 m). To determine a characteristic wind strength in such a case, we start from velocity time series $U(t)$ measured at some altitude. As shown by Ungar and Haff

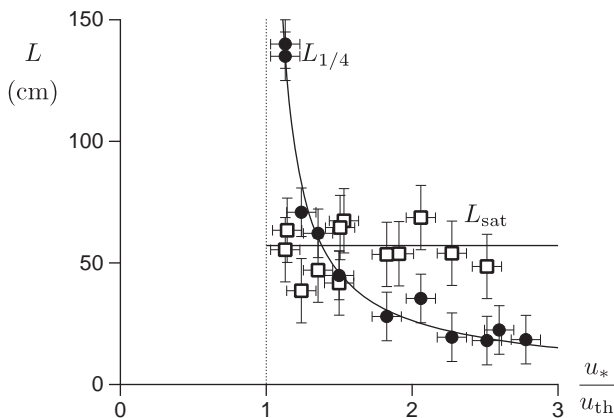


Fig. 3. Direct measurements of the saturation length L_{sat} (\square) and of the ejection length $L_{1/4}$ (\bullet) as a function of the wind shear velocity u_* , rescaled by the threshold u_{th} . By definition, $L_{1/4}$ is the length needed before the flux q reaches $q_{\text{sat}}/4$; L_{sat} is the relaxation length close to the saturated state. The solid lines are respectively the best fit by a constant and by a power law diverging at the threshold.

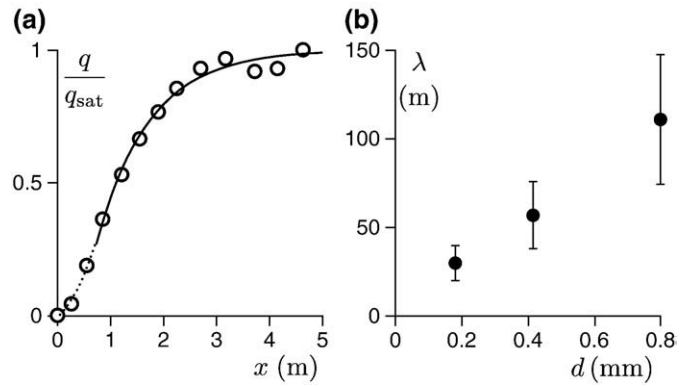


Fig. 4. (a) Spatial variation of the sediment flux over a flat sand bed measured in the field by Elbelrhiti et al. (2005) for $d = 185 \mu\text{m}$ and $u_* \sim 1.3 u_{\text{th}}$. (b) Length of the proto-dunes (see the photograph in Fig. 6(f)) from Atlantic Sahara with sand of different mean diameters d covering the dune surface.

(1987) and Andreotti (2004), the saturated flux q_{sat} is proportional to $(U^2 - U_{\text{th}}^2) \mathcal{H}(U - U_{\text{th}})$, where U_{th} is the threshold value for transport, and where $\mathcal{H}(x)$ is the so-called Heaviside function [$\mathcal{H}(x > 0) = 1$ and $\mathcal{H}(x < 0) = 0$]. We then define the effective velocity as that which would give the same mean flux, if the wind was not fluctuating:

$$\left(\frac{u_*}{u_{\text{th}}}\right)^2 = 1 + \left\langle \left[\left(\frac{U(t)}{U_{\text{th}}}\right)^2 - 1 \right] \mathcal{H}(U(t) - U_{\text{th}}) \right\rangle, \quad (3)$$

where the term $\langle \dots \rangle$ denotes an average over time. Interestingly, the ratio so defined does not depend on the height above the bed at which the anemometer is placed, which justifies that it is also the ratio of the typical shear velocity u_* to its threshold value u_{th} . For this particular measurement, we find $u_* \approx 1.3u_{\text{th}}$.

3. Initial dune wavelength

In the second part of this paper, we investigate the relation between the saturation length and the size at which dunes form. This relation dates back to the pioneering works by Bagnold (1941) who was the first to point out the existence of a minimal dune size. This is particularly obvious in barchan fields, like those of the Atlantic Sahara where we have been doing field measurements for eight years: dunes only present a slip face when they are larger than a length λ . We call proto-dunes, the dunes that present vanishing slip faces over long periods of time (see pictures in Fig. 6d–f). Most of the barchans of the Atlantic Sahara are composed of sand of mean diameter $d = 180 \mu\text{m}$. Still, one can observe, at different places, proto-barchans covered by coarser grains. Fig. 4b shows the relation between the length λ of these proto-dunes and the grain size. They are subjected to the very same wind conditions. One observes that this minimal size increases roughly linearly with the grain diameter d . How is the sand transport saturation length, on the order of one meter (Fig. 4a), related to the size at which dunes form, which is typically few tens of meters (Fig. 4b)?

The theoretical prediction of the wavelength at which dunes emerge from a flat sand bed has been progressively refined since the first linear stability analysis of Andreotti et al. (2002). It is based on two separate stages. First, one needs to perform the hydrodynamical calculation of the turbulent velocity field around obstacles of small amplitude (Jackson and Hunt, 1975; Richards, 1980; Hunt et al., 1988). One extracts from these calculations the components of the basal shear stress in phase and in quadrature with the elevation profile, as a function of the ratio of the wavelength λ to the aerodynamical roughness z_0 . The most detailed calculation has been performed by Fourrière et al. (2010). In particular, the robustness of the results with respect to the turbulence modeling has been

systematically tested. Second, one needs to describe the sand transport around the saturated state. The initial stage of the saturation is transient, dominated by the ejection of new grains is thus irrelevant to the problem of dune formation. It turns out that the results – in particular the prediction of the emerging wavelength – are not sensitive to the formula used for the transport law that relates the saturated flux to the basal shear velocity. We have used here the scaling law derived by Ungar and Haff (1987) and Andreotti (2004): $q_{\text{sat}} \propto (u_*^2 - u_{\text{th}}^2)$. To use this formula correctly, the threshold shear velocity must depend on the sand bed slope $\partial_x h \equiv \tan \varphi$. Following Iversen and Rasmussen (1994, 1999), we write the dependence in the form $u_{\text{th}}^2(\varphi) = u_{\text{th}}^2(0)(\cos \varphi + \sin \varphi / \mu)$. These authors have found values of μ slightly larger than the avalanche slipface slope. Using our field measurements, we fixed this value to $\mu = \tan(32^\circ)$. Then, one needs a model for the aerodynamic roughness z_0 induced by sand transport. Consistently with our choice for the sand transport, we use the result obtained by Ungar and Haff (1987) on the existence of a ‘focal point’ at which the wind velocity profiles obtained at different shear velocities cross at a single point. On this basis, Andreotti (2004) has derived the relation between z_0 and u_* . The velocity and the height of the focal point as a function of the grain size d are determined from the data of Rasmussen et al. (1996). Finally, one has to choose the saturation length L_{sat} . The wavelength λ at which dunes form is then entirely determined. Let us emphasize that the components of the model are robustly determined, except L_{sat} – this is precisely our purpose here. The solid line in Fig. 5 shows the relation between the wavelength and the rescaled shear velocity u_*/u_{th} for a constant value of L_{sat} . At high wind, the wavelength tends to a constant, proportional to L_{sat} . Close to the threshold, the stabilizing effect of the slope (parameter μ) makes the wavelength λ increase.

Conversely, one can use the wavelength as an indirect way to measure the saturation length. In this inverse problem, we determine the value L_{sat} such that the fastest growing wavelength corresponds to that measured. Given that the instability requires typically 100 m to develop, wind tunnels cannot be used to form dunes under controlled conditions. Fortunately, the surface of large dunes precisely behave as flat areas of sand and are thus subjected to the primary linear instability (Elbelrhiti et al., 2005). The main difficulty is to assess the wind velocity associated with the formation of given superimposed bedforms. Fig. 6a shows a situation in which this can be achieved rigorously. Indeed, the superimposed bedforms of wavelength λ on the stoss slope of this barchan dune are transverse to the dune itself. They are formed by a strong storm almost perpendicular to the regular trade winds ($\theta = 23^\circ$ to the North) blowing over the Atlantic Sahara

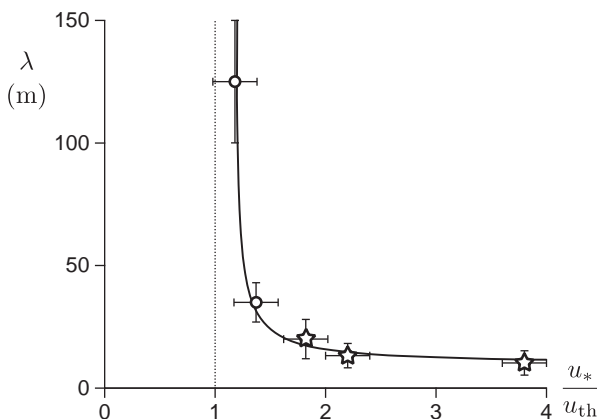


Fig. 5. Measured most unstable wavelength λ as a function of the rescaled wind shear velocity u_*/u_{th} , for a mean grain size $d \approx 185 \mu\text{m}$. The star symbols (\star) correspond to superimposed structures on barchans generated by stormy events. The circles (\circ) correspond to low amplitude transverse dunes generated by averaged winds. The solid line corresponds to the predictions of the model described in the text, for a constant saturation length $L_{\text{sat}} \approx 70 \text{ cm}$.

(Fig. 6b). This hot and dry anomalous wind, called ‘Chergui’, is due to the motion of the Azores anticyclone over Europe and generates dust jets over the ocean. Figs. 6b,c show the two successive storms of this type, both characterised by a peak of wind velocity and a rotation of the wind direction. We have analyzed several such events, which occur between 5 and 10 times per year and are presumably responsible for a part of the dynamics of barchan fields (Hersen et al., 2004; Elbelrhiti et al. 2008). Importantly, we were present in the field during some of these storms and have been able to observe the resulting bed instability. In order to determine the most unstable wavelength, we have averaged the spacing between secondary bedforms over typically 20 barchan dunes. The wind velocity is consistently determined on the crest of dunes, taking into account the speed-up factor ~ 1.4 (Andreotti et al., 2002) with respect to the wind strength over the surrounding flat ground (Fig. 6c). It is averaged over the period of time during which the wind blows in the direction perpendicular to the new-born crests, following Eq. (3). This procedure allows to obtain data (stars in Fig. 5) far above the transport threshold (from $1.5u_{\text{th}}$ to $4u_{\text{th}}$), since the selected events should be strong enough to destabilise the surface of dunes within a few days. In this range of wind velocity, the most unstable wavelength λ_{max} is largely independent of u_* .

Seeking for situations closer to the threshold of transport, we have investigated the case of dunes that present vanishing avalanche slip faces. Fig. 6 shows transverse dunes of this type, in northwestern Ar-Rub-Alkhali (Saudi Arabia). They are composed of grains of size $d \approx 190 \mu\text{m}$ (Abolkhair, 1986), i.e. comparable to those in the Atlantic Sahara. We hypothesise that these small amplitude dunes remain at the wavelength at which a flat sand bed destabilises. They can be considered as being subjected to the average wind at the scale of the year, as defined by Eq. (3). One finds a mean wavelength $\lambda = 130 \text{ m}$ in Ar-Rub-Alkhali, while the same pattern in the Atlantic Sahara rather presents a smaller wavelength $\lambda = 35 \text{ m}$. Analysing time-series of the velocity measured in the airports surrounding these dune fields, it turns out that the characteristic wind shear velocity is significantly smaller in the former ($u \sim 1.2u_{\text{th}}$) than in the later ($u \sim 1.4u_{\text{th}}$) location. Because of the assumption made, these two points (circles in Fig. 5) are less reliable than those measured after the destabilisation induced by a clearly identified wind event. Still, two independent observations make us confident that the large wavelength observed in northwestern Ar-Rub-Alkhali is not due to a pattern coarsening process. First, we do not observe there any superimposed bedforms. Second, at the margin of the transverse dune field, there is evidence of isolated dunes in an intermediate state between slipfaceless dome dunes and well developed barchans. This is clearly the signature of a proto-dune close to the minimal length of dunes (Hersen et al., 2002; Kroy et al., 2002; Andreotti and Claudin, 2007; Parteli et al., 2007). In Ar-Rub-Alkhali, they can be as large as 220 m, which is ~ 7 times larger than in the Atlantic Sahara (compare panels (e) and (f) of Fig. 6). This confirms the sharp increase of the most unstable wavelength close to the transport threshold (Fig. 5).

In summary, based on the comprehensive linear stability analysis whose components have been summarized above, we have solved the inverse problem and converted the data $\lambda(u_*/u_{\text{th}})$ into a relation between L_{sat} and u_*/u_{th} (Fourrière et al., 2010). Fig. 7 shows that this independent determination of L_{sat} is in fair agreement with the direct one, once properly rescaled: L_{sat} is around $2(\rho_s/\rho_f)d$, within a 50% dispersion. In particular, one cannot observe any particular trend of the data to increase or decrease. It means that the decrease of the emerging wavelength observed in Fig. 5 can be entirely ascribed to the slope (gravity) effect.

4. Concluding remarks

In this paper, we have presented accurate measurements of the sand transport saturation length L_{sat} . Both direct and indirect methods consistently show that L_{sat} is mostly independent on the wind

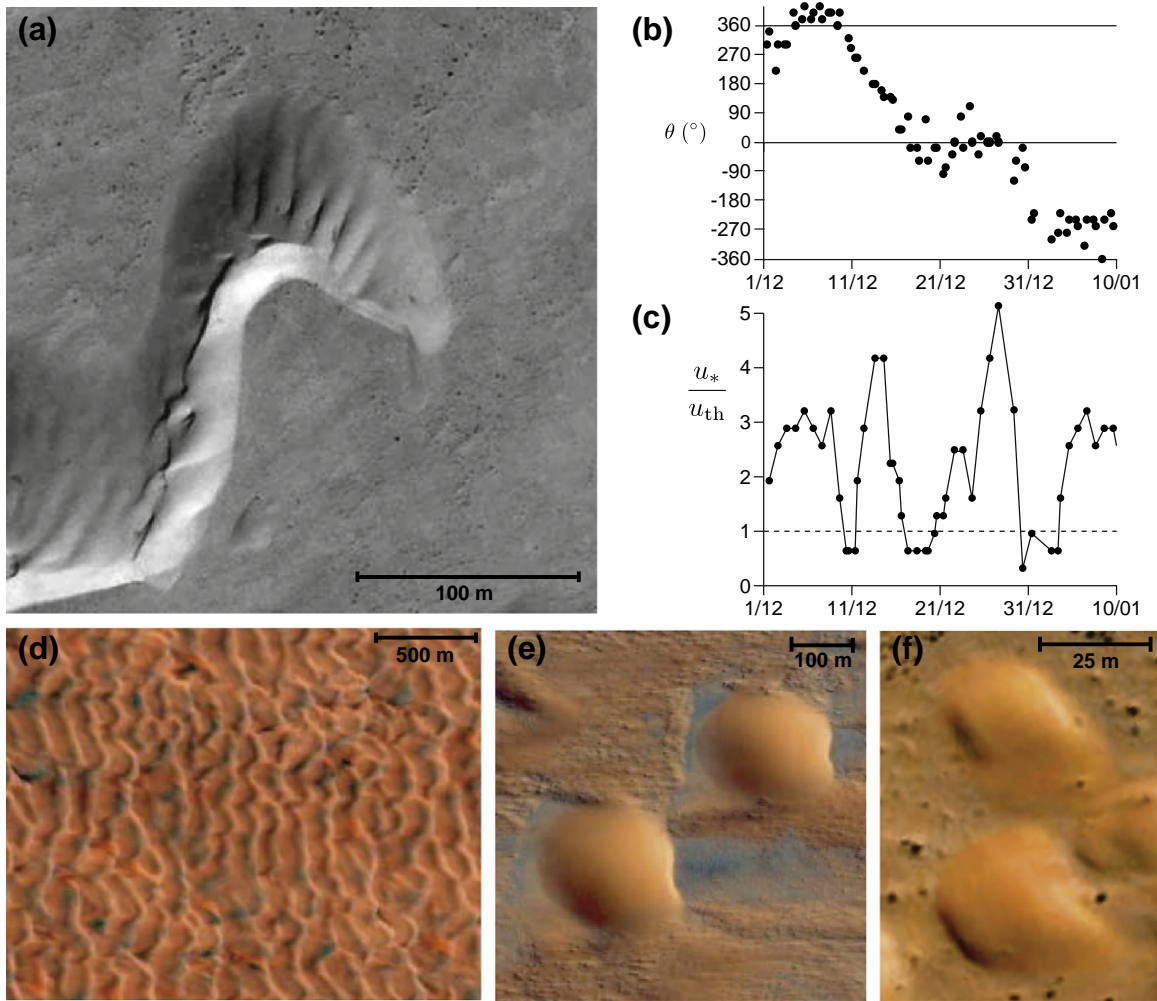


Fig. 6. (a) Barchan instability in the Atlantic Sahara due to a storm characterised by a strong dry wind coming from inland (Chergui). Aerial photograph taken on January the 5th, 2005 – credits DigitalGlobe. (b) Wind direction, with respect to the North, measured in Tan-Tan between December the 1st, 2004, and January the 10th, 2005 – regular trade winds are along $\theta \approx 23^\circ$. (c) Corresponding values of the basal shear velocity u_* . (d) Aerial picture of a transverse dune field in Northwestern Ar-Rub-Alkhali (S. Arabia). (e) 220 m long proto-dunes in Northwestern Ar-Rub-Alkhali (S. Arabia) (typical local wind: $u_* \sim 1.2 u_{th}$). (f) 30 m long proto-dunes in the Atlantic Sahara (typical local wind: $u_* \sim 1.4 u_{th}$).

strength – in the range of velocities investigated – and rescales well with the drag length $\rho_s/\rho_f d$. This result strongly supports the interpretation that grain inertia is the dominant dynamical mechanism limiting sediment transport saturation on dunes. Note that, at saturation, the grain hop length and height must also be independent of u_* , so that it is in fact difficult to distinguish between inertia and saltating effects.

Clearly, this first order relaxation process only captures the processes involved into the spatial evolution of the sand flux close

to the saturated state but misses the initial increase of q . Interestingly, this initial stage is very sensitive to the wind shear velocity, and thus must be related to other mechanisms. A complete theory including both initial and saturated regimes is then desirable. For this purpose, new experiments and simulations investigating both components of the sand flux (grain density as well as grain velocity) are required. Also, higher wind velocities should be explored.

Acknowledgements

We wish to thank F. Naaim and the ETNA group of the Cemagref in Grenoble for the use of their wind tunnel and for their kind help during the experiments. This work has benefited from the support of the Agence Nationale de la Recherche, grant ‘Zephyr’ (#ERCS07 18), and of the ‘Institut Universitaire de France’.

References

Abolkhair, Y.M., 1986. The statistical analysis of the sand grain size distribution of Al-Ubay-lah barchan dunes, Northwestern Ar-Rub-Alkhali desert. S. Arabia. *GeoJournal* 13, 103–109.
 Andreotti, B., 2004. A two species model of aeolian sand transport. *J. Fluid Mech.* 510, 47–70.
 Andreotti, B., Claudin, P., 2007. Comment on ‘Minimal size of a barchan dune’. *Phys. Rev. E* 76, 063301.
 Andreotti, B., Claudin, P., Douady, S., 2002. Selection of dune shapes and velocities (2 Parts). *Eur. Phys. J. B* 28, 321–339. *Eur. Phys. J. B* 28, 341–352.

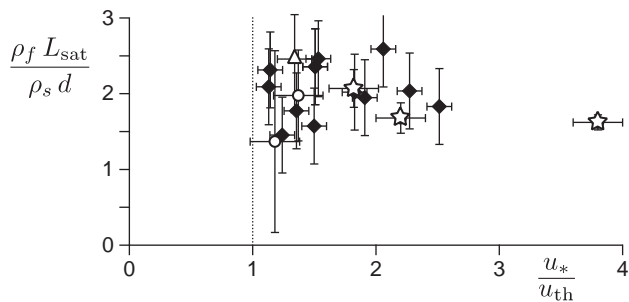


Fig. 7. Saturation length L_{sat} , rescaled by the drag length $\rho_s/\rho_f d$, as a function of the wind shear velocity u_* , rescaled by the threshold u_{th} . Direct measurements, performed in a wind tunnel (\blacklozenge) and in the field (\triangle), are compared to those determined from the initial dune wavelength (storms: \star) and slipfaceless dunes (\circ).

- Bagnold, R.A., 1941. *The Physics of blown sand and desert dunes*. Chapman and Hall, London.
- Charru, F., 2006. Selection of the ripple length on a granular bed. *Phys. Fluids* 18, 121508.
- Cierco, F.-X., Naaim, M., Naaim-Bouvet, F., 2008. Experimental study of particle concentration fluctuations in a turbulent steady flow. *Ann. Glaciol.* 49, 121–126.
- Claudin, P., Andreotti, B., 2006. A scaling law for aeolian dunes on Mars, Venus, Earth, and for subaqueous ripples. *Earth Planet. Sci. Lett.* 252, 30–44.
- Creysse, M., Dupont, P., Ould el Moctar, A., Valance, A., Cantat, I., Jenkins, J.T., Pasini, J.M., Rasmussen, K.R., 2009. Saltating particles in a turbulent boundary layer: experiment and theory. *J. Fluid Mech.* 625, 47–74.
- Dong, Z., Wang, H., Liu, X., Wang, X., 2004. The blown sand flux over a sandy surface: a wind tunnel investigation of the fetch effect. *Geomorphology* 57, 117–127.
- Elbelrhiti, H., Claudin, P., Andreotti, B., 2005. Field evidence for surface-wave-induced instability of sand dunes. *Nature* 437, 720–723.
- Elbelrhiti, H., Andreotti, B., Claudin, P., 2008. Barchan dune corridors: field characterization and investigation of control parameters. *J. Geophys. Res.* 113, F02S15.
- Fourrière, A., Claudin, P., Andreotti, B., 2010. Bedforms in a turbulent stream: formation of ripples by primary linear instability and of dunes by non-linear pattern coarsening. *J. Fluid Mech.* 649, 287.
- Gilette, D.A., Herbert, G., Stokton, P.H., Owen, P.R., 1996. Causes of the fetch effect in wind erosion. *Earth Surf. Process. Land.* 21, 641–659.
- Hersen, P., Douady, S., Andreotti, B., 2002. Relevant lengthscale of barchan dunes. *Phys. Rev. Lett.* 89, 264301.
- Hersen, P., Elbelrhiti, H., Andersen, K.H., Andreotti, B., Claudin, P., Douady, S., 2004. Corridors of barchan dunes: stability and size selection. *Phys. Rev. E* 69, 011304.
- Hunt, J.C.R., Leibovich, S., Richards, K.J., 1988. Turbulent shear flows over low hills. *Q. J. R. Meteorol. Soc.* 114, 1435–1470.
- Iversen, J.D., Rasmussen, K.R., 1994. The effect of surface slope on saltation threshold. *Sedimentology* 41, 721–728.
- Iversen, J.D., Rasmussen, K.R., 1999. The effect of wind speed and bed slope on sand transport. *Sedimentology* 46, 723–731.
- Jackson, P.S., Hunt, J.C.R., 1975. Turbulent wind flow over a low hill. *Q. J. R. Meteorol. Soc.* 101, 929–955.
- Kroy, K., Sauer mann, G., Herrmann, H.J., 2002. Minimal model for sand dunes. *Phys. Rev. Lett.* 88, 054301. Minimal model for aeolian sand dunes. *Phys. Rev. E* 66, 031302.
- Lancaster, N., Nickling, W.G., McKenna-Neuman, C.K., Wyatt, V.E., 1996. Sediment flux and airflow on the stoss slope of a barchan dune. *Geomorphology* 17, 55–62.
- Liu, X., Dong, Z., 2004. Experimental investigation of the concentration profile of a blowing sand cloud. *Geomorphology* 60, 371–381.
- McKenna-Neuman, C., Lancaster, N., Nickling, W.G., 1997. Relations between dune morphology, air flow, and sediment flux on reversing dunes, Silver Peak, Nevada. *Sedimentology* 44, 1103–1113.
- Owen, P.R., 1964. Saltation of uniform grains in air. *J. Fluid Mech.* 20, 225–242.
- Parteli, E.J.R., Durán, O., Herrmann, H.J., 2007. Minimal size of a barchan dune. *Phys. Rev. E* 75, 011301. Reply to comment on 'Minimal size of a barchan dune'. *Phys. Rev. E* 76, 063302.
- Rasmussen, K.R., Iversen, J.D., Rautahaimo, P., 1996. Saltation and wind flow interaction in a variable slope wind tunnel. *Geomorphology* 17, 19–28.
- Richards, K.J., 1980. The formation of ripples and dunes on an erodible bed. *J. Fluid Mech.* 99, 597–618.
- Sauer mann, G., Kroy, K., Herrmann, H.J., 2001. A phenomenological dynamic saltation model for dune formation. *Phys. Rev. E* 64, 031305.
- Ungar, J.E., Haff, P.K., 1987. Steady state saltation in air. *Sedimentology* 34, 289–299.
- Wiggs, G.F.S., Livingstone, I., Warren, A., 1996. The role of streamline curvature in sand dune dynamics: evidence from field and wind tunnel measurements. *Geomorphology* 17, 29–46.